Rapid Communication in Photoscience (2016), vol. 5, no. 2, pp. 18-20
http://dx.doi.org/10.5857/RCP.2016.5.2.18 ISSN 2288-4564(Online)

Communication

Quantum Chemistry Based Arguments about Singlet Oxygen Formation Trends from Fluorescent Proteins

Jae Woo Park and Young Min Rhee*

Department of Chemistry, Pohang University of Science and Technology (POSTECH), Pohang 37673, Korea

ABSTRACT: Through quantum chemical means, we inspect the energetics of the singlet oxygen formation with fluorescent proteins in their triplet excited states. By placing an oxygen molecule at varying distances, we discover that the energetic driving force for the singlet oxygen formation does not depend strongly on the chromophore – O_2 distance. We also observe that the chromophore vibrations contribute much to the energy gap modulation toward the surface crossing. Based on our computational results, we try to draw a series of rationalizations of different photostabilities of different fluorescent proteins. Most prominently, we argue that the chance of encountering a surface crossing point is higher with a protein with a lower photostability.

Fluorescent proteins (FPs) have become one of the most important molecular imaging tools for various biological systems.[1-9] There are many recently developed FPs with different emission wavelengths, quantum yields, and fluorescence lifetimes.[6-14] Indeed, one important issue in the applications of FPs is their photostabilities, which have direct relationships with their photobleaching characters.[2-7] Thus, many researchers have struggled toward developing FP variants with improved photostabilities.[6,7,10-12] This photostability feature will be the target of main discussion in this communication.

It has been known that photobleaching of FPs is related to singlet oxygen generated by their chromophore.[5] When singlet oxygen is formed, it chemically attacks the protein and induces photobleaching. We can assume that singlet oxygen is generated by the interaction between molecular oxygen and the chromophore in its triplet excited state,[4] namely

$$T^* + {}^3O_2 \rightarrow S + {}^1O_2 \quad (1)$$

However, the details of this process are not well understood yet. Understanding this pathway of singlet oxygen formation will thus help toward further developing FPs with different photobleaching properties.

Reaction (1) will occur when two potential energy surfaces, $T^* + {}^3O_2$ (triplet + ${}^3\Sigma_g^-$; "triplet+triplet" hereafter) and $S + {}^1O_2$ (singlet + ${}^1\Sigma_g^+$; "singlet+singlet" hereafter), cross with each other. Of course, this surface crossing will appear along a seam in the conformation space and have some dependence on the oxygen – chromophore distance, which we will inspect first. We will then show that this surface crossing and the subsequent singlet oxygen formation dominantly depends on the chromophore configuration. Based on these, we will try to explain the dependence of photobleaching properties on the fluorophore structure.

For this, the structures of singlet and triplet GFP model chromophore, *p*-hydroxybenzylideneimidazoline (*p*HBI) and molecular oxygen was optimized at the M06-2X[15]/6-311+G(d,p) level of theory. To investigate the dependence of energy on the position of molecular oxygen, we have generated chromophore geometries with diverse oxygen configurations. An oxygen molecule was placed in a parallel manner with respect to the molecular plane of *p*HBI with varying molecular distances from 3.0 Å to 10.0 Å. For these geometries, the energies of adiabatic triplet+triplet and singlet+singlet states were calculated at the SA4-CAS(6,5)SCF[16] level with the 6-31G(d) basis set. In addition, the role of the internal conformational motion of GFP, BFP, and CFP chromophores were inspected by adopting *ab initio* molecular dynamics (AIMD) and single-point multi-configurational calculations. The energy gradients for AIMD simulations were calculated at the M06-2X/6-31G(d) level of theory with initial velocities randomly generated for 600 K temperature. The simulations were run for 500,000 a.u. (~12 ps) with 50 a.u. of time step. The snapshots for multi-configurational single-point energy calculations were collected at every 5000 a.u. (~120 fs). Thus, at any given O_2–chromophore distance, there were 100 conformations from AIMD toward statistical treatments. All bonds involving hydrogen atoms were constrained with the RATTLE algorithm.[17] The single-point energies of adiabatic states were calculated at the SA4-MR-CAS(6,5)PT2[18]/6-31G(d) level. The geometry optimizations and AIMD simulations were performed using developers' version of Q-Chem 3.2 package.[19] All other calculations were carried out with MOLPRO.[20]

The energetics of FP model chromophores calculated with M06-2X/6-311+G(d,p) are listed in Table 1. Indeed, the optimized triplet+triplet energy is higher than the singlet+singlet one, meaning that Reaction (1) will be thermodynamically spontaneous.

Table 1. Energetics of Reaction (1), in kJ/mol units.

		GFP	BFP	CFP
Reactants	${}^3O_2$	0.00	0.00	0.00
	T_1	166.64	177.98	176.94
Products	${}^1O_2$	156.43	156.43	156.43
	S_0	0.00	0.00	0.00
Exothermicity		10.21	21.55	20.51

***To whom correspondence should be addressed.**
E-mail: ymrhee@postech.ac.kr

Figure 1 shows the energy averages and standard deviations in the two states at various chromophore to oxygen distances for the GFP case. For the GFP chromophore, we performed MCSCF calculations for the chromophore – oxygen geometries generated as described in the above part, and defined the inter-molecular distance as the shortest of all atom-to-atom distances. Two chromophore conformations were adopted for simulations toward generating this figure: Figure 1(a) is from the M06-2X optimized geometry, and Figure 1(b) is from the geometry with the lowest observed energy and with nearly-degenerate singlet+singlet and triplet+triplet states. In both cases, we can see that the fluctuations of state energies (represented by standard deviations) increase at shorter chromophore – O_2 distances. This is natural as the orbitals of the two molecules interact more strongly at a closer distance. The standard deviations (σ's) of the energies, which reflect the vibrational energy fluctuations, are quite similar in (a) and (b), which is again natural. However, as the energy gap closes in as in Figure 1(b) at distances shorter than 5.0 Å, σ overwhelms the energy gap. In addition, the gap energy (the gap between the red and the blue lines) has only a weak dependence on the chromophore – O_2 distance. From these aspects, we can infer that the configurational variations of the chromophore play a dominant role in determining the surface crossing nature and the overall dynamics of the systems.

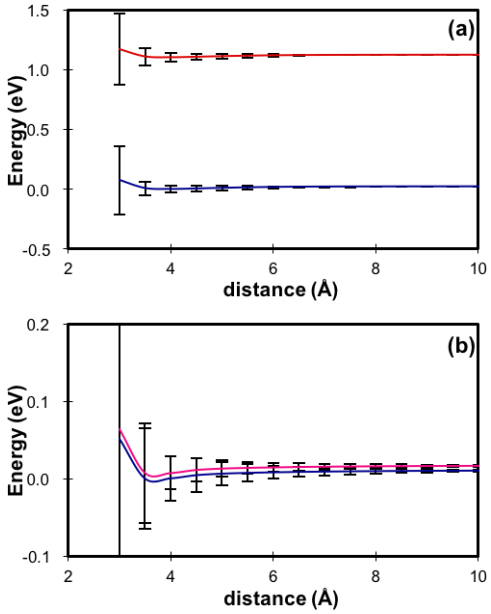

Figure 1. Average energies (lines) and standard deviations (error bars) of the singlet+singlet (blue) and triplet+triplet (red) states as functions of the chromophore to oxygen distance for GFP, obtained with geometry ensembles starting (a) from a ground state optimized geometry and (b) from a surface intersecting geometry.

Now, let us investigate how frequently the two surfaces cross in different "real" FPs. The photobleaching time scales of EGFP, ECFP, and EBFP are about 150 s, 50 s and 1 s.[6,7,10,11] As described in a previous section, we performed AIMD simulations for GFP, CFP, and BFP chromophore units. Based on the fact that the energy varied insensitively with the chromophore – O_2 separation, we took 100 snapshots from each chromophore and added O_2 molecular to each snapshot and then performed single point CASPT2 calculations. Figure 2 shows the histogram of the energy gaps between the involved two states. One can see that the energy gap is larger with GFP than with CFP or with BFP. Despite their higher excitation or fluorescence energy (namely, the larger S_0 – S_1 gap) of the chromophore, interestingly, the energy differences between two spin-exchanging states are smaller with bluer FPs. This feature stems from the fact that the gap between chromophore T_1 and S_1 states is also larger in BFP / CFP. From this, we can imagine that triple oxygen will cross over to singlet state more often. This is in line with the fact that GFP is more photostable than CFP and BFP.

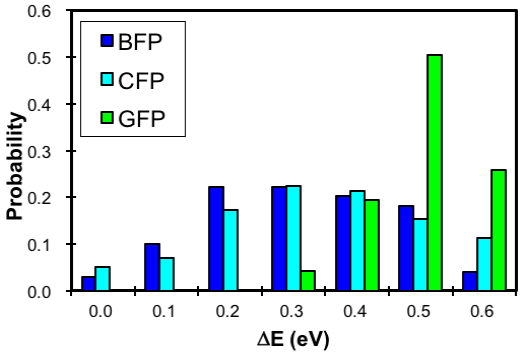

Figure 2. Histograms of the energy gaps between the triplet+triplet and the singlet+singlet states obtained with geometry ensembles from dynamics simulations.

Of course, as can be easily inferred from Figure 1, this $^3O_2$ to $^1O_2$ conversion will take place when the oxygen molecule is in close proximity with the chromophore, likely inside the protein barrel structure. Indeed, researchers have explained that the shielding from oxygen diffusion is a key factor behind high photostability.[9,21] Similarly, a reduction of the volume of the accessible space around the chromophore will give rise to a photostability increase by decreasing the number of oxygen molecules near the chromophore. For example, major mutation sites in azurite[10] and EBFP2.0,[11] the BFP variants with ~100-fold increases in photostability, are close to the chromophore and do not appear to change the barrel structure toward hindering oxygen diffusion. Perhaps, this fact can also be used for justifying the photostability difference between BFP and CFP. Chromophore units of both proteins showed a similar frequency of approaching regions of lower energy gaps (Figure 2). However, the CFP chromophore is bulkier than the BFP chromophore due to its Y66W mutation, leading to an effectively smaller cavity size.

In conclusion, we have inspected the energetics of the singlet oxygen formation around triplet-excited FP chromophore with quantum chemical means. From our approach of scanning the oxygen locations, even though it was quite crude and approximate in its nature, we have argued that the energetic driving force for the spin-exchange type of reaction does not depend strongly on the chromophore – O_2 distance, and that the chromophore vibrations contribute much to the energy gap modulation. By performing CASPT2 calculations combined with AIMD simulations, we tried to draw a series of rationalizations of different photostabilities of different fluorescent proteins. The results suggested, at least weakly, that the chance of encountering surface crossing points is higher with proteins with lower photostabilities. We also note that the singlet oxygen formation and the related photobleaching are governed by many complicated factors. They are definitely affected by the chromophore characteristics, but at the same time by diffusion-blocking by the tight β-barrel and space-accessibility inside the cavity around the chromophore. Theoretical approaches with atomic resolutions can indeed be powerful tools toward understanding such

complicated physical aspects, and they will surely be helpful in performing related future investigations especially when they are carried out in a careful manner against many possible difficulties related to excited state treatments.

Received September 17, 2016; Accepted October 4, 2016.

KEYWORDS: fluorescent protein, quantum chemistry, molecular dynamics

ACKNOWLEDGEMENT

The authors are grateful for the supercomputer time from Korea Institute of Science and Technology Information (KISTI).

REFERENCES AND NOTES

1. van Thor, J. J. *Chem. Soc. Rev.* **2009**, *38*, 2935.
2. Tsien, R. Y. *Annu. Rev. Biochem.* **1998**, *67*, 509.
3. Meech, S. R. *Chem. Soc. Rev.* **2009**, *38*, 2922.
4. Diaspro, A.; Chirico, G.; Usai, C.; Ramoino, P.; Dobrucki, J., Photobleaching. In *Handbook of Biological Confocal Microscopy*, Springer: 2006.
5. Greenbaum, L.; Rothmann, C.; Lavie, R.; Malik, Z. *Biol. Chem.* **2000**, *381*, 1251.
6. Shaner, N. C.; Patterson, G. H.; Davidson, M. W. *J. Cell Sci.* **2007**, *120*, 4247.
7. Shaner, N. C.; Steinbach, P. A.; Tsien, R. Y. *Nat. Meth.* **2005**, *2*, 905.
8. Day, R. N.; Davidson, M. W. *Chem. Soc. Rev.* **2009**, *38*, 2887.
9. Chapagain, P. P.; Regmi, C. K.; Castillo, W. *J. Chem. Phys.* **2011**, *135*, 235101.
10. Mena, M. A.; Treynor, T. P.; Mayo, S. L.; Daugherty, P. S. *Nat. Biotechnol.* **2006**, *24*, 1569.
11. Ai, H.-W.; Shaner, N. C.; Cheng, Z.; Tsien, R. Y.; Campbell, R. E. *Biochemistry* **2007**, *46*, 5904.
12. Ai, H.-W.; Henderson, J. N.; Remington, S. J.; Campbell, R. E. *Biochem. J.* **2006**, *400*, 531.
13. Remington, S. J. *Curr. Opin. Struct. Biol.* **2006**, *16*, 714.
14. Pakhomov, A. A.; Martynov, V. I. *Chem. Biol.* **2008**, *15*, 755.
15. Zhao, Y.; Truhlar, D. G. *Theor. Chem. Acc.* **2008**, *120*, 215.
16. Stålring, J.; Bernhardsson, A.; Lindh, R. *Mol. Phys.* **2001**, *99*, 103.
17. Andersen, H. C. *J. Comput. Phys.* **1983**, *52*, 24.
18. Finley, J.; Malmqvist, P.-Å.; Roos, B. O.; Serrano-Andrés, L. *Chem. Phys. Lett.* **1998**, *288*, 299.
19. Shao, Y.; et al. *Phys. Chem. Chem. Phys.* **2006**, *8*, 3172.
20. MOLPRO, version 2009.1, a package of ab initio programs, Werner, H.-J.; et al. (http://www.molpro.net).
21. Campbell, R. E.; Tour, O.; Palmer, A. E.; Steinbach, P. A.; Baird, G. S.; Zacharias, D. A.; Tsien, R. Y. *Proc. Natl. Acad. Sci. U.S.A.* **2002**, *99*, 7877.
22. Rhee, Y. M.; Park, J. W. *Int. J. Quantum Chem.* **2016**, *116*, 573.